Investigation of microsphere-mediated cellular delivery by chemical, microscopic and gene expression analysis

Investigation of microsphere-mediated cellular delivery by chemical, microscopic and gene expression analysis†

Lois M. Alexander,‡[a] Salvatore Pernagallo,‡[a] Alessandra Livigni,[b] Rosario M. Sánchez-Martín,[a] Joshua M. Brickman[b] and Mark Bradley*[a]

Received 20th July 2009, Accepted 22nd October 2009
First published as an Advance Article on the web 26th November 2009
DOI: 10.1039/b914428e

Amino functionalised cross-linked polystyrene microspheres of well defined sizes (0.2–2 μm) have been prepared and shown to be efficient and controllable delivery devices, capable of transporting anything from small dye molecules to bulky proteins into cells. However, the specific mechanism of cellular entry is largely unknown and widely variant from study to study. As such, chemical, biological and microscopic methods are used to elucidate the mechanism of cellular uptake for polystyrene microspheres of 0.2, 0.5 and 2 μm in mouse melanoma cells. Uptake is found to be wholly unreliant upon energetic processes, while lysosomal and endosomal tracking agents failed to show co-localisation with lysosomes/endosomes, suggesting a non-endocytic uptake pathway. To further explore the consequences of microsphere uptake, gene expression profiling is used to determine if there is a transcriptional response to ''beadfection'' in both murine and human cells. None of the common transcriptional responses to enhanced endocytosis are observed in beadfected cells, further supporting a non-endocytic uptake mechanism. Furthermore, the microspheres are noted to have a limited interaction with cells at a transcriptional level, supporting them as a non-toxic delivery vehicle.

Introduction

The development of cellular delivery devices, which includes cationic lipids, cell penetrating peptides (CPP's) and nanotubes and have been used to deliver anything from small dye molecules to large RNAs[1–3] into cells, has become a topic of zealous interest within the research community.

Some of the major hurdles that need to be overcome in order to develop an efficient delivery vehicle are ease of cargo loading to the delivery device, efficiency of delivery to the cytoplasmic region of the cell and controllability of cellular loading. However, a number of widely used delivery vehicles can have substantial, undesired cytotoxic effects, limiting their widespread use.[4,5]

In contrast, polymeric microspheres have been repeatedly demonstrated to be non-toxic and effective tools for cell biology, flow cytometry and medical diagnostics.[6–8] In addition, microspheres are able to enter a wide range of cell lines with high, but controllable loadings and can be easily functionalised with a range of moieties.

Despite the widespread utility of microspheres, the mechanism of microsphere uptake by non-phagocytic cells is poorly understood.[9] In general, two main uptake mechanisms may be considered: active endocytic processes[10] and/or passive diffusive mechanisms.[11] Insertion into the lipid bilayer and diffusion to the intracellular environment have previously been suggested for carbon nanotubes, amongst other mechanisms, after finding sodium azide, an inhibitor of adenosine triphosphate (ATP) hydrolysis, had a limited effect on uptake.[12] While some data support the notion that commercially available microspheres are taken up endocytically,[9,10,13,14] it is hard to reconcile this when their capacity to function as cytoplasmatic pH and calcium sensors has been demonstrated.[15,16] Microspheres have also been used to deliver siRNA intracellularly for the efficient gene silencing

[a] *Chemical Biology Section, School of Chemistry, University of Edinburgh, West Mains Road, Edinburgh, UK EH9 3JJ. E-mail: mark.bradley@ed.ac.uk; Fax: +44 (0)131 650 6453; Tel: +44 (0)131 651 3307*
[b] *MRC Center for Regenerative Medicine, Institute for Stem Cell Research, University of Edinburgh, West Mains Road, Edinburgh, UK EH9 3JJ*

† Electronic supplementary information (ESI) available: Fig. S1 shows the uptake of 2, 0.5 and 0.2 μm fluorescein microspheres by B16F10, E14 mES, HEK293T, HeLa, K562 and L929 cells as a function of time. Fig. S2 shows cellular viability by MTT assay following 24 hours incubation with microspheres. Fig. S3 shows the uptake of 2, 0.5 and 0.2 μm fluorescein microspheres by E14 mES, HEK293T, HeLa and L929 cells following treatment with 20 mM sodium azide. Fig. S4 shows the uptake of LacCer and transferrin controls under caveolae and clathrin-mediated endocytosis inhibition. Fig. S5 shows beadfected B16F10 cells pre-treated with mβ-CD and lovastatin. Fig. S6 shows cellular viability by MTT assay following treatment of B16F10 cells with chemical inhibitors. Fig. S7 shows beadfected B16F10 cells pre-treated with filipin III and genistein. Fig. S8 shows beadfected B16F10 cells pre-treated with chlorpromazine or under potassium depletion. Fig. S9 shows beadfected B16F10 cells pre-treated with DMA. Fig. S10 shows the uptake in B16F10 cells pre-treated with nocodazole. Fig. S11 shows real-time microscopy stills of a B16F10 cell ingesting 0.5 μm microspheres. Fig. S12 shows microscopy of cells treated with lysotracker red and microspheres. Fig. S13 shows the uptake of 2 and 0.5 μm microspheres in L929 and HEK293T cells after 48 hours and the cellular viability by MTT assay. Two real-time movies. Microarray data deposition: gene expression data have been deposited in ArrayExpress EBI (Experiment name: Bradley-Group_Microspheres for Cellular Delivery; ArrayExpress accession: E-MEXP-1845). See DOI: 10.1039/b914428e

‡ These authors contributed equally to this work.

of enhanced green fluorescent protein (EGFP) and functional proteins, such as β-galactosidase, which both require cytoplasmic localisation.[17,18] Taken together, these observations are inconsistent with an uptake mechanism that involves traditional endocytosis.

In this paper, the uptake of microspheres in several different cell lines was investigated as a function of microsphere diameter (0.2, 0.5 and 2 μm) and time of incubation (6–24 hours). Interestingly, microsphere uptake was found to be widely dependent on the microsphere diameter, with some cells taking up one size of microsphere better than others, with no logical patterns emerging. While these observations do not support endocytosis, this mechanism was investigated by both chemical modulation and sub-cellular localisation studies.

Microarray analysis was also used to determine whether significant gene expression changes occur in response to beadfection.[19,20] In particular, we show that there were no significant changes that occurred in response to microsphere uptake and that these changes did not include any of the known transcriptional responses to endocytosis. Moreover, this analysis showed no significant changes in genes associated with cell death using larger sized microspheres, suggesting that beads represent a highly effective, non-toxic method for cellular delivery.

Results

Cellular uptake of polystyrene microspheres

Uniform, monodisperse polystyrene amino-functionalised cross-linked microspheres (Fig. 1a and b) were synthesised by dispersion polymerisation as described previously, and coupled to different fluorophores as shown in Fig. 1c.[21]

In order to assess the uptake and toxicity patterns of 0.2, 0.5 and 2 μm amino-functionalised cross-linked polystyrene microspheres, and to assess their applicability as cellular delivery devices, fluorescein-conjugated microspheres were incubated with a range of cell lines (mouse melanoma (B16F10), human cervical cancer (HeLa), human embryonic kidney (HEK293T), mouse fibroblast (L929), erythroleukemic (K562) and feeder independent mouse embryonic stem cells (E14Tg2A)). As well as examining cell line dependence, microsphere uptake was assessed as a function of microsphere diameter (0.2, 0.5 or 2 μm) by flow cytometry (Fig. 2 upper).

Microsphere uptake was also confirmed by microscopy (Fig. 2a–c lower) and found to be high across all cell lines (approaching 95%), especially with use of the smaller sized microspheres (0.2 and 0.5 μm). Unsurprisingly, cellular uptake was also found to be time dependent, with longer incubations yielding higher uptakes across all sizes of microsphere (see Fig. S1 in ESI†).

To confirm that microsphere uptake did not affect viability in this range of cell lines, 3-(4,5-dimethylthiazol-2-yl)-2,5-diphenyltetrazolium bromide (MTT) cellular viability assays were used to estimate the percentage of viable cells in these cultures following treatment with a range of microspheres. Fig. S2 in ESI† shows that all cell lines contained greater than 90% viable cells following microsphere treatment, indicating that microspheres did not exert any cytotoxic effects on cells.

Chemical inhibition of uptake pathways

Uptake of microspheres is not energy dependent. Active mechanisms such as endocytosis are dependent on an energy source such as adenosine triphosphate (ATP).[22] If levels of ATP are depleted in cells then active mechanisms are consequently inhibited.[23] It was therefore examined whether microsphere uptake was energy dependent by incubating microspheres with cells that had been pre-treated with an inhibitor of ATP production, sodium azide (20 mM), which is known to block endocytosis.

Uptake of microspheres was measured by flow cytometry in 0.2% trypan blue in Hank's balanced saline solution (HBSS), designed to quench extracellular fluorescence so only cells containing microspheres intracellularly were detectable.[10,24]Fig. 3a shows that pre-treatment of cells with sodium azide had no effect on the uptake of microspheres in mouse melanoma B16F10 cells. Similar results were obtained with all other cell lines tested (see Fig. S3 in ESI†). In contrast, the uptake of FITC-conjugated transferrin and

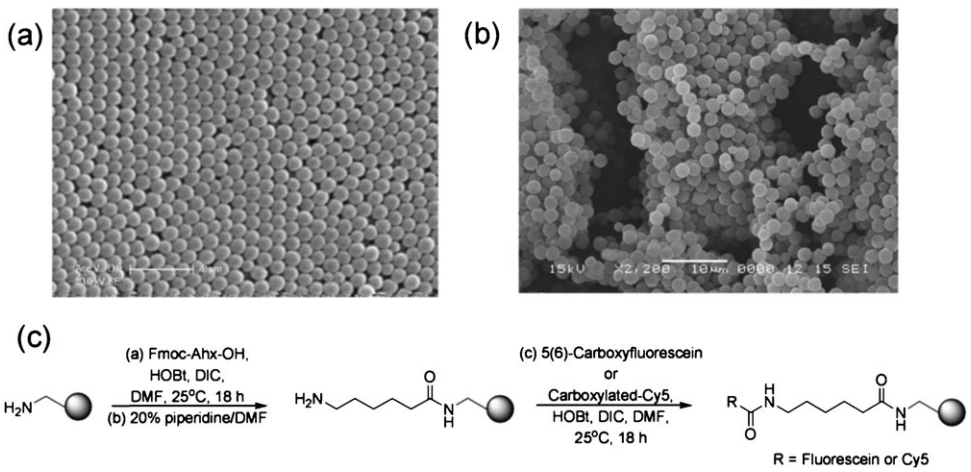

Fig. 1 Preparation of amino-functionalised polystyrene microspheres. Scanning electron microscopy images of (a) 0.5 μm and (b) 2 μm microspheres. (c) Chemical coupling of fluorescent dyes (fluorescein and Cy5) onto the microspheres. Fluorophore-coupled microspheres were prepared *via* an aminohexanoic unit to limit steric interactions and improve bioavailability.

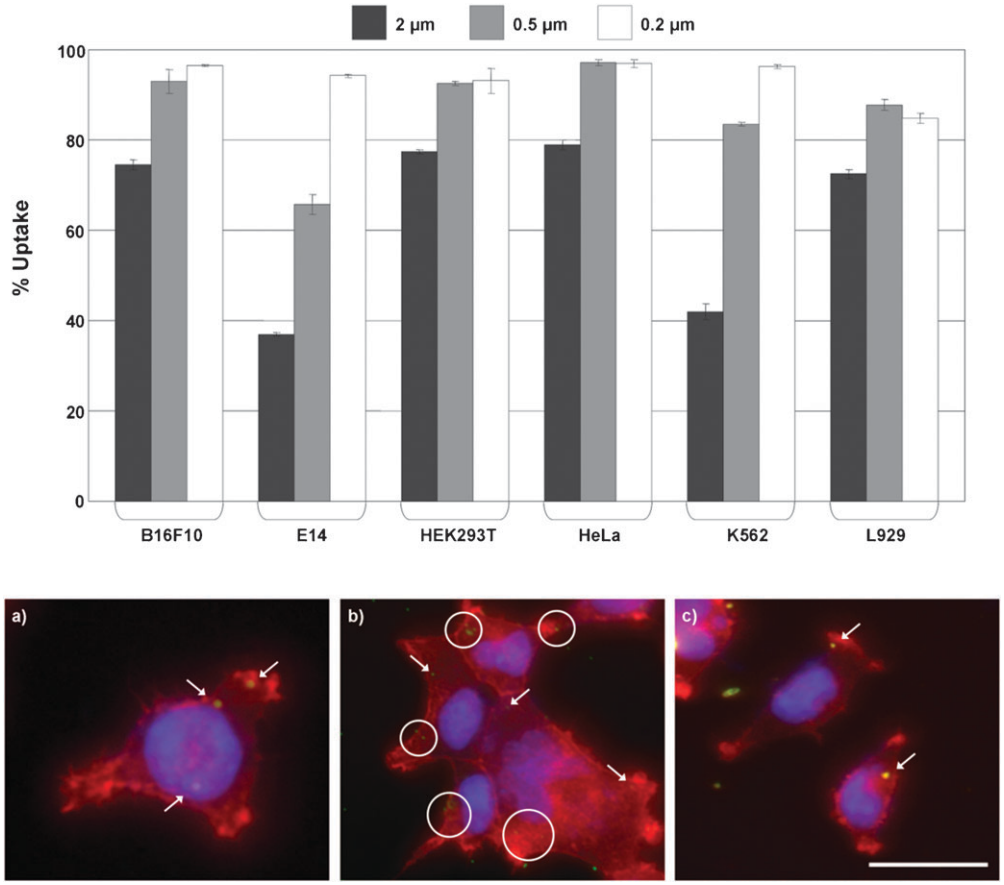

Fig. 2 Uptake of 2, 0.5 and 0.2 μm fluorescein labelled microspheres by cells. Top: uptake measured by flow cytometry after 24 h in B16F10, E14, HEK293T, HeLa, K562 and L929 cells (% uptake is the % of the total population containing microspheres where 0% is untreated cells). Bottom: images of B16F10 cells with: (a) 2 μm fluorescein microspheres; (b) 0.5 μm fluorescein microspheres; (c) 0.2 μm fluorescein microspheres. Actin filaments are stained with AlexaFluor 568-phalloidin and the cell nuclei are stained with Hoechst 33 342. Scale bar is 25 μm.

BODIPY-labeled lactosyl ceramide (LacCer), which are known to be ingested by receptor-mediated endocytosis, was inhibited under these conditions (see Fig. S4 in ESI†).

The presence of cholesterol in the cellular membrane is also essential for energy dependent endocytosis and, as such, its depletion results in a general block on endocytic mechanisms.[25] We therefore sought to confirm that microsphere uptake was not reliant upon the presence of cholesterol by incubating microspheres with cells grown in a cocktail of cholesterol inhibitors that included mβ-cyclodextrin (mβ-CD) (to remove cholesterol already present in the membrane)[26] and lovastatin (to prevent the *de novo* synthesis of further cholesterol by inhibition of 3-hydroxy-3-methyl-glutaryl-CoA reductase).[25] Following pre-incubation of cells with mβ-CD (10 mM) and lovastatin (1 μg mL^{-1}), 0.2, 0.5 and 2 μm fluorescein microspheres were added and uptake was analysed by flow cytometry after 3 hours. Fig. 3b shows that incubation with these cholesterol inhibitors does not hinder microsphere uptake, while identical conditions blocked the endocytic uptake of both LacCer and transferrin. Microsphere uptake

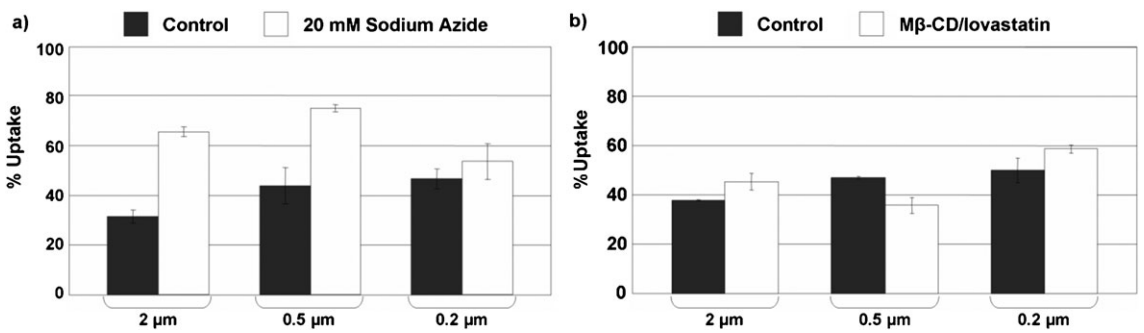

Fig. 3 Effect of ATP and cholesterol depletion on microsphere uptake. Uptake of 2, 0.5 and 0.2 μm fluorescein microspheres in B16F10 cells after 3 hours of (a) ATP depletion with sodium azide (20 mM); (b) cholesterol depletion with mβ-CD (10 mM) and lovastatin (1 μg mL^{-1}).

was additionally confirmed by microscopy (see Fig. S5 in ESI†), while MTT toxicity assays were undertaken to confirm mβ-CD and lovastatin did not significantly affect the number of viable, proliferating cells in these cultures (see Fig. S6 in ESI†).

Uptake of microspheres is not reliant upon caveolae. Although uptake was not found to be either ATP or cholesterol dependent, it was important to ensure that the uptake of microspheres did not occur by any form of endocytosis. As such, caveolae-mediated endocytosis, a mechanism known to be responsible for the uptake of LacCer, was selectively inhibited by the use of filipin III and genistein. Filipin III inhibits caveolae-mediated endocytosis by sequestering cholesterol in lipid rafts, which are essential for caveolae formation,[27] while genistein inhibits caveolae-mediated endocytosis by inhibiting a tyrosine kinase, which is required to phosphorylate proteins involved in caveolae formation.[28] B16F10 cells were incubated with filipin III (5 μg mL^{-1}) and genistein (200 μM), concentrations sufficient to inhibit the uptake of BODIPY FL C_5-lactosylceramide (LacCer)[29] (see Fig. S4 in ESI†), prior to the addition of microspheres. Fig. 4a shows that the uptake of microspheres by these cells, in which all caveolae-mediated endocytosis was blocked, was the same as in untreated cultures (measured by flow cytometry), demonstrating that caveolae-mediated endocytosis was unlikely to be responsible for microsphere entry in B16F10 cells.

Uptake was additionally confirmed by microscopy (see Fig. S7 in ESI†) and, as above, MTT assays were used to show that these inhibitors had no effect on cell viability at the doses used (see Fig. S6 in ESI†).

Uptake of microspheres is not reliant upon clathrin. As caveolae-mediated invaginations into the cellular membrane are generally 50–100 nm in diameter,[30] it may not be surprising that microspheres 4 to 40 times larger than these regions are not ingested *via* this mechanism. However, clathrin-mediated endocytosis can result in the formation of widely size variant endosomes, which are largely dependent on the cargo to be internalised.[31]

Clathrin-mediated endocytosis can be inhibited by chlorpromazine or depletion of potassium levels, known to disrupt the clathrin-mediated pathway by preventing coated pit assembly.[31,32] Inhibitor doses were established such that the endocytosis of FITC-conjugated transferrin was blocked[33] (see Fig. S4 in ESI†). Strikingly, cells that could not endocytose transferrin were still capable of taking up microspheres (Fig. 4b), indicating that clathrin coated pits were unlikely to be responsible for microsphere uptake (microscopy confirmed microsphere uptake under clathrin-coated pit inhibition, see Fig. S8 in ESI†). MTT assays showed that culturing cells under these conditions had little effect on the number of viable cells (see Fig. S6 in ESI†).

Uptake of microspheres is not reliant upon macropinocytosis. We also considered non-specific endocytic pathways, such as macropinocytosis, whereby a ruffling-like procedure by the cell membrane results in the formation of a vesicle, which may subsequently be internalised.[34] Membrane ruffling can be inhibited in two ways. Dimethylamiloride (DMA), an inhibitor of Na^+–H^+ exchange, blocks macropinocytosis by altering the concentrations of sodium ions, which are thought to be important to non-specific membrane ruffling. Alternatively, the underlying morphological rearrangements can be blocked by inhibiting F-actin elongation with cytochalasin D.

The effect of both these inhibitors on the uptake of microspheres (0.2, 0.5 and 2 μm) by B16F10 cells was analysed and quantified by flow cytometry and microscopy (Fig. 5 and Fig. S9 in ESI†). Interestingly, while DMA had little effect on microsphere uptake, cytochalasin D reduced microsphere uptake by 2–3-fold. Thus, while it appears unlikely that microspheres enter cells by macropinocytosis, there appears at least a partial requirement for actin polymerisation in the uptake process. This would suggest that uptake could involve some level of cytoskeletal rearrangement or may require an intact actin network for microsphere–cell interactions.

Uptake of microspheres is not reliant upon microtubule polymerisation. As actin polymerisation appeared relevant to uptake, the assessment of other cytoskeletal rearrangements known to be implicated in endocytosis was important. Lipid raft-mediated uptake and intracellular vesicular trafficking are thought to be dependent upon microtubule polymerisation and are blocked by nocodazole.[35] The capacity of nocodazole to inhibit microsphere uptake in B16F10 cells was therefore assessed. As with the other endocytosis inhibitors, nocodazole had little effect on microsphere uptake (see Fig. S10 in ESI†), suggesting that microtubule polymerisation is not required for either the interaction of the microspheres with the cellular membrane or their passage across the lipid bilayer. Thus

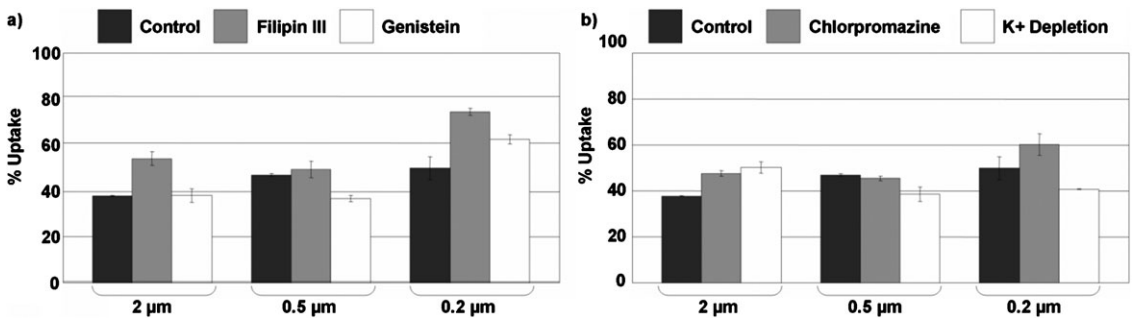

Fig. 4 Effect of inhibition on caveolae and clathrin-mediated endocytosis. Uptake of 2, 0.5 and 0.2 μm microspheres by B16F10 cells with a blockade on (a) caveolae-mediated endocytosis with filipin III (5 μg mL^{-1}) and genistein (200 μM); (b) clathrin-mediated endocytosis with potassium depletion (see Materials for buffer constituents) and chlorpromazine (10 μg mL^{-1}).

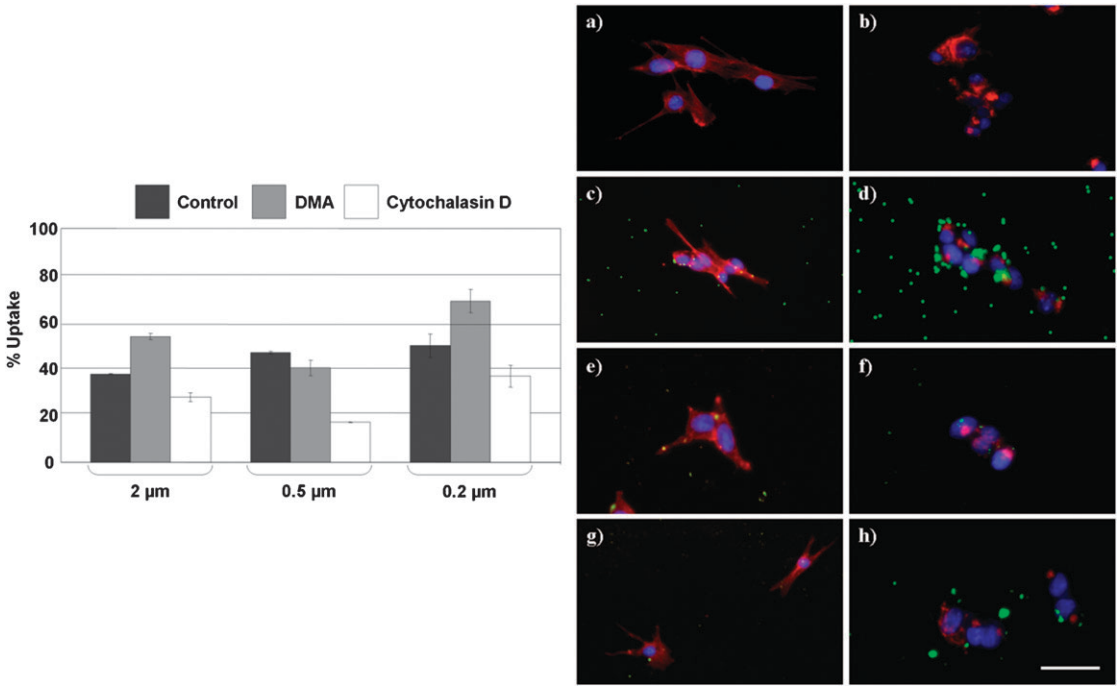

Fig. 5 Effect of macropinocytosis inhibition. Uptake of 2, 0.5 and 0.2 μm microspheres by B16F10 cells unable to undergo macropinocytosis. Left: DMA (10 μM) or cytochalasin D (10 μM) (% uptake is the % of the total population containing microspheres where 0% beadfection is untreated cell); right: microscopy of cells under standard incubation conditions (a, c, e and g) and in the presence of cytochalasin D (10 μM) (b, d, f and h). (a) and (b) are control cells with no microspheres; (c) and (d) are with 2 μm FAM-beads; (e) and (f) are with 0.5 μm FAM-beads; (g) and (h) are with 0.2 μm FAM-beads. Actin filaments are stained with AlexaFluor 568-phalloidin and the cell nuclei are stained with Hoechst 33 342. Scale bar is 140 μm.

despite a requirement for F-actin elongation and an intact cytoskeleton, lipid raft-mediated uptake is unlikely to be the mechanism by which microspheres are internalised.

Temperature dependence on uptake

Low temperatures have a substantial effect on cellular uptake processes, including endocytosis and passive diffusive mechanisms.[36] "Hardening" of the lipid bilayer at lowered temperatures would be expected to slow passive diffusive mechanisms due to increased membrane rigidity.[37] To examine the temperature dependence on uptake, B16F10 cells were incubated at 37, 20 and 4 °C and entry of microspheres into the cells was assessed after 3 hours by flow cytometry and microscopy (Fig. 6). In all cases, uptake was dramatically lowered at 20 °C and the effect was even more pronounced at 4 °C. At these low temperatures, microspheres do not extensively enter cells, but rather appear anchored to the cell membrane (Fig. 6a–c). Taken together with our inhibitor studies, these data suggest that the reduction in uptake is due to hardening of the lipid bilayer and a decrease in membrane fluidity, meaning passive movement across the membrane is hindered.

Endosomal and lysosomal markers

Although chemical inhibition of endocytic pathways had little effect on microsphere uptake, it is difficult to wholly rule out this mechanism. To further test whether microsphere uptake was in some way tied to endocytosis, the sub-cellular co-localisation of microspheres with endosomal and lysosomal markers was examined. FM4-64 is a commercially available lipophilic styryl dye, which through anchorage into the lipid bilayer labels the membrane of the cell and any subsequently formed endosomal compartments.[38] B16F10 mouse melanoma cells were pre-incubated with FM4-64 followed by 0.5 μm fluorescein microspheres and real-time confocal analysis carried out over a period of 30 minutes (see ESI† for the real-time movies).

Three microspheres were observed to have become anchored with the extracellular region of the cell and after repeated re-orientation of their alignment, the microspheres (still associated with one another) crossed the lipid bilayer rapidly and without the appearance of an endosome (see Fig. S11 in ESI†). However, disruption of the membrane was noted and evidenced by the association of the FM4-64 stain to one side of the microspheres, which gradually disassociated with time (it was no longer present after 15 minutes within the cell). Thus, microspheres appear to locally disrupt the membrane upon entering the cell and this observation would explain the reduction in uptake induced by inhibiting actin polymerisation.

To further confirm that this passage across the cell membrane does not result in lysosomal compartmentalisation, it was considered whether internalised microspheres co-localised with acidic organelles (lysosomes) following uptake.

As such, B16F10 cells were stained with LysoTracker Red, a dye capable of marking acidic compartments,[39] and analysed by confocal microscopy.

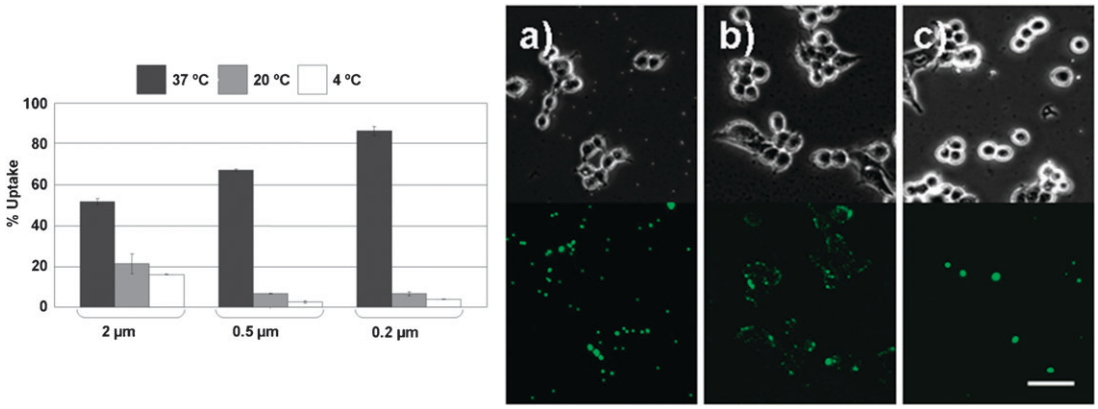

Fig. 6 Effect of temperature. Uptake of 2, 0.5 and 0.2 μm microspheres by B16F10 cells. Left: flow cytometry after 3 hours incubation; right: microscopy of cells with: (a) 2 μm microspheres incubated at 20 °C; (b) 0.5 μm microspheres incubated at 20 °C; (c) 0.2 μm microspheres incubated at 20 °C. Top are overlay images and bottom are fluorescence images. Scale bar is 300 μm.

Optical sections through cells containing internalised microspheres demonstrated that microspheres did not co-localise with lysosomes (Fig. 7 and Fig. S12 in ESI†), further supporting a mechanism which is not related to endocytosis.

Gene expression profiling

To further investigate the effect of microspheres on cells, the transcriptional consequences of uptake were analysed using gene profiling technology.[40] Agilent 4 × 44K whole human and mouse genome arrays were used to assess changes in gene expression levels that occurred as a result of the uptake of two differently sized microspheres (2 and 0.5 μm) in both mouse (L929 fibroblast) and human (HEK293T human embryonic kidney) cell lines. Transcriptional responses were examined in the hope of uncovering any significant and conserved changes in gene expression following beadfection (see Fig. S13 in ESI†).

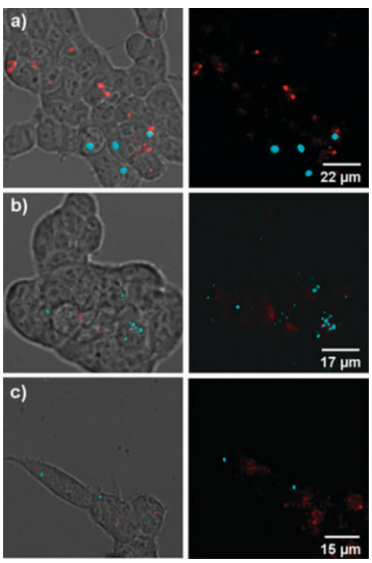

Fig. 7 Lysosomal staining. B16F10 cells incubated with Cy5 labelled microspheres (a) 2 μm; (b) 0.5 μm and (c) 0.2 μm microspheres (cyan) followed by LysoTracker Red (red). Images were collected on a Zeiss inverted confocal DM IRE2 microscope.

Preliminary analysis focused on the individual effect of microsphere size (0.5 or 2 μm) on HEK293T or L929 cells (see Tables SI–SIV in ESI†). In human HEK293T cells only 11 genes showed a greater than 2-fold expression change in response to 0.5 μm microspheres, while 21 genes changed their expression levels upon beadfection with 2 μm beads. In addition, only 5 genes were found to be in common between the two profiles (beadfection with 0.5 μm or beadfection with 2 μm).

Similar results were obtained with mouse L929 cells in which the expression levels of 28 genes were found to change in response to 0.5 μm microspheres and 13 genes were found to be up or down-regulated in response to 2 μm microspheres. In this case, only 3 genes were found to be common between the two sizes of microsphere. Strikingly, very few gene expression changes occurred upon treatment with either bead size, demonstrating how well tolerated the microspheres are by the cell. In addition, the genes altered were not conserved between species and significant homology was not evident.

To find any common changes between the two cell lines a more general analysis was performed, grouping the datasets irrespective of the microsphere diameter. In HEK293T cells, 38 genes appeared to be differentially expressed with over a 2-fold change in response to microsphere uptake, whereas, in mouse L929 cells, the expression levels of 74 genes were found to be altered (Fig. 8 and Tables SV and SVI in ESI†).

However, even with this less stringent approach the expression of only a small set of genes was found to change as a result of microsphere uptake and no homology could be found between the cell lines.

To determine if there were any core processes affected by microsphere uptake, gene ontology analysis was used to study their roles in biological processes that might be contained within any transcriptional response. In L929 cells, this confirmed that the addition of microspheres had no effect on cellular viability as the genes affected by beadfection were mainly related to cellular metabolism (Fig. 9, right). However, in HEK293T cells 2 genes out of 38 were noted to be involved in apoptosis or cell cycle arrest (Fig. 9, left), demonstrating the more sensitive nature of this cell line to beads over-loading.

Importantly, gene ontology analysis of both cell types generated results consistent with the chemical inhibitory

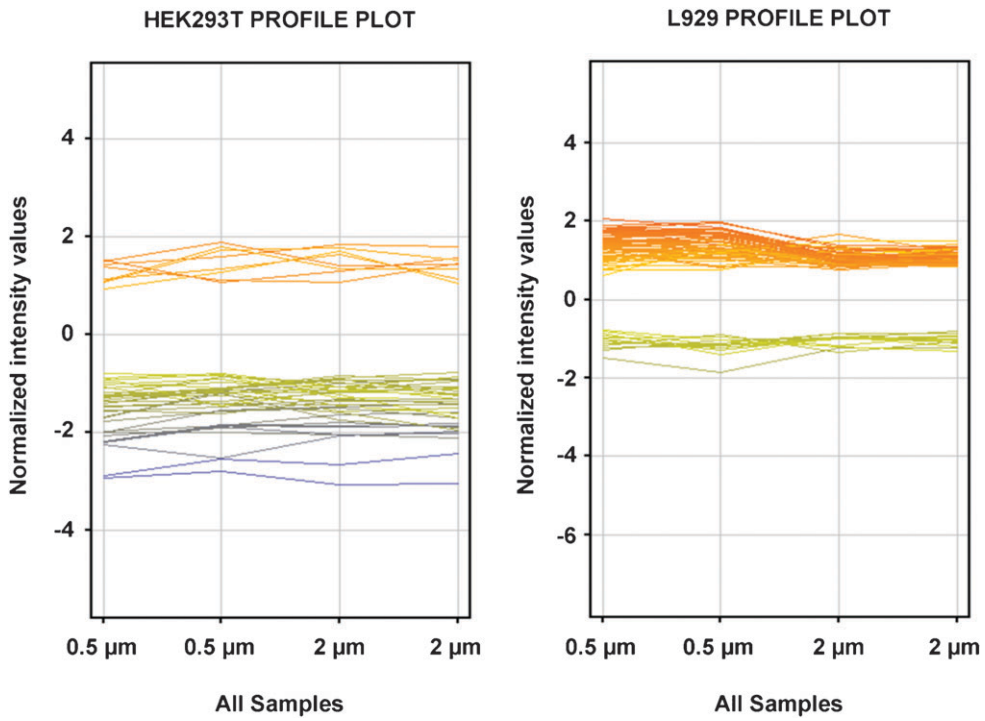

Fig. 8 Gene expression profiling. Profile plots of up and down-regulated genes across the 4 samples (normalised values in $\log_2$ scale). Analysis was made on four different subarrays. '0.5 µm' corresponds to subarrays hybridised with total RNA obtained from cells grown with 0.5 µm microspheres and '2 µm' corresponds to subarrays hybridised with total RNA obtained from cells grown with 2 µm microspheres.

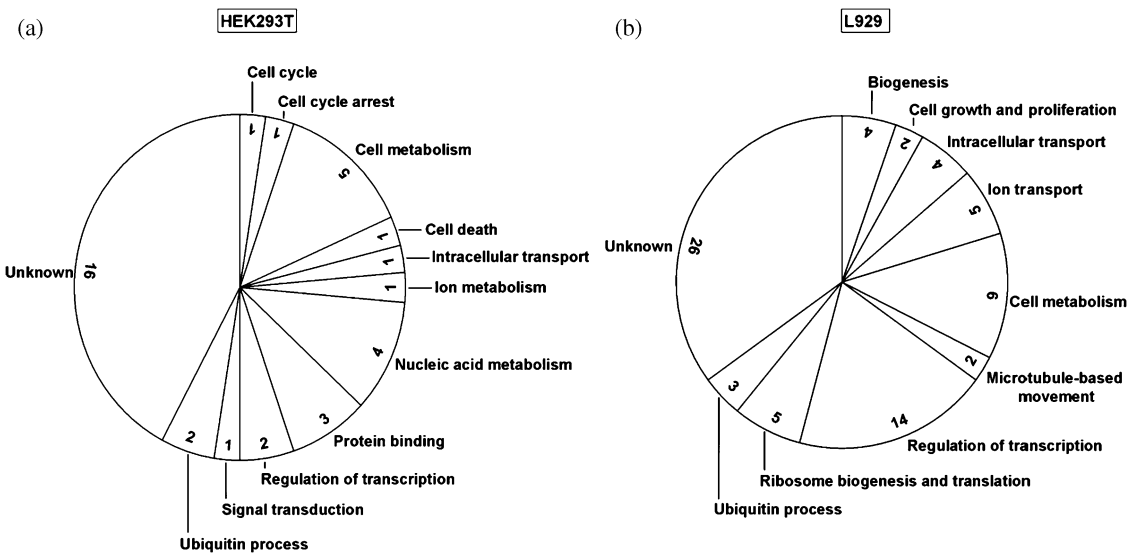

Fig. 9 Gene ontology. Pie graphs of gene ontology analysis. (a) HEK293T gene function of the 38 genes appeared to be differentially expressed with over a 2-fold change in response to the microspheres; (b) L929 cells, gene function of 74 genes found to be altered with a 2-fold change in the expression levels.

assays and microscopic analysis as none of the gene expression changes induced by microsphere uptake resembles those expected as a result of endocytosis.

Data validation

As no conserved patterns were observed in response to microsphere uptake, it appeared that both cell lines remained essentially unchanged in response to beadfection.

To confirm that these transcriptional profiles were accurate, the few statistically significant changes were validated by quantitative real-time PCR analysis. Transcripts showing a greater than 3-fold change in expression levels on the array chip were selected for further analysis (see Table SVII in ESI†). Independent biological samples from cells treated with microspheres under the same conditions, described for the microarray study, were used and a comparison was made

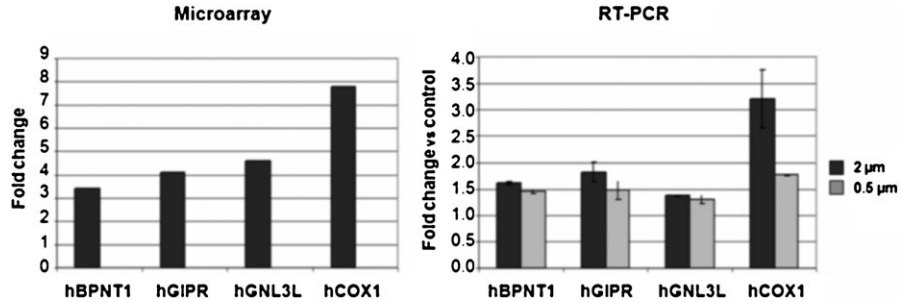

Fig. 10 Data validation. Comparison of the gene expression fold changes from microarray analysis (left panel) and quantitative real-time RT-PCR (right panel). For the real-time assay, HEK293T cells were incubated with 0.5 μm (grey) and 2 μm (black) microspheres. The *y*-axis represents the fold change relative to the untreated control cells. The transcripts number is normalised relative to human β-actin. The fold change value represents the mean of 2 experiments.

between the microarray and the quantitative PCR results (Fig. 10). In accordance with the microarray data, all the genes examined were found to be up-regulated in cells incubated with microspheres, although, overall, the fold changes seen were less dramatic than predicted by the microarray, however, the relative abundance of the transcripts was conserved.

None of the gene expression changes appear conserved between human and murine cell lines. The restricted number of transcripts moderately up-regulated in response to microsphere uptake having a role in metabolism, biogenesis and cell homeostasis. For example gastric inhibitory polypeptide receptor (GIPR) is a G-protein coupled receptor normally expressed in the fetal kidney and involved in glucose homeostasis.[41] Guanine nucleotide binding protein-like 3 (GNL3L) is a GTP-binding chaperone involved in ribosome biogenesis.[42] BPNT1 (bisphosphate 3′-nucleotidase) is a magnesium-dependent phosphomonoesterase that converts 3′(2′)-phosphoadenosine-5′-phosphate (PAP) to AMP, thus playing a role in nucleotide metabolism.[43] COX-1 (cytochrome oxidase subunit I)[44] is a mitochondrial transcript which encodes one of the major transmembrane subunits of cytochrome C oxidase, the last enzyme in the respiratory chain.

Discussion

In this paper, microspheres within a biologically relevant size range (0.2–2 μm) were shown to represent a highly efficient delivery system in a wide variety of cell lines, including mouse stem cells. The uptake of these microspheres was found to be size and time dependent (although cellular entry was high in all cases), but is independent of active transport. Moreover, the ingestion of these particles neither appears to impact on cell viability nor produce any significant changes in gene expression. As a result microspheres appear to represent a highly efficient, biologically inert delivery system.

Investigation of microsphere uptake was studied initially by chemical modulation and was found to be independent of both ATP and cholesterol depletion (both required for endocytosis). Moreover, a number of inhibitors were examined designed to block receptor-mediated (clathrin- or caveolae-mediated) endocytosis and they were found to have no impact on microsphere uptake at concentrations that significantly inhibited LacCer and transferrin uptake. Whilst these findings supported a non-endocytic mechanism, one inhibitor did appear to impact on uptake. Cytochalasin D, an inhibitor of F-actin polymerisation, yielded a decrease in uptake of up to 60% and microscopy revealed that microspheres could be seen to be 'sitting' on extracellular regions of the cells, unable to pass intracellularly. These observations suggest that microsphere uptake may require modulation of the actin cytoskeleton, in a process that does not require ATP hydrolysis.

Importantly, examination of the gene expression profile induced by microsphere uptake revealed no significant transcriptional changes in comparison to untreated control cells. Analysis performed using less stringent criteria identified small changes in a reduced number of transcripts (n = 38 and 74). Gene ontology of these subsets evidenced that none were typical transcriptional responses to endocytosis, further supporting a non-endocytic pathway.

Based on the absence of evidence for some form of endocytotic pathway, coupled to the requirement for actin polymerisation, we propose a mechanism whereby microspheres interact and anchor with the cell membrane. After a period of time that is dependant on bead microsphere diameter and cell line, membrane reorganisation occurs, facilitating the influx of the microsphere intracellularly. Such a mechanism must be wholly unreliant upon an energetic payload and would not result in the trapping of cargo within acidic organelles or result in cytotoxicity. As such, this renders microspheres as not only an efficient delivery vehicle, but also a device which may have wide ranging and versatile applications in a great number of areas of research.

Experimental procedures

Materials

Cellular uptake was assessed by flow cytometry using a BD Bioscience FACSAria equipped with the FACSDiva software. Cellular microscopy was performed on a Zeiss Axiovert 200M pseudo confocal microscope or a Leica inverted-confocal microscope and real-time microscopy was performed on a DeltaVision microscope. Real-time PCR was performed using a LightCycler 480 (Roche, UK) and a LightCycler 480 SYBR Green 1 Master (Roche, UK).

Styrene and *p*-divinylbenzene (DVB) were purchased from Sigma-Aldrich and *tert*-butylcatechol removed by washing

with 25% NaOH followed by water. 4-Vinylbenzylamine (VBAH) was prepared in-house from 4-vinylbenzylchloride (Sigma-Aldrich) as we have previously reported.[21] All other chemicals were used as received. Roswell Park Memorial Institute Medium (RPMI-CM) and Dulbecco's Modified Eagle Medium (DMEM) were purchased from Sigma-Aldrich and supplemented with 10% fetal bovine serum, 100 units per mL penicillin/streptomycin and 4 mM L-glutamine unless otherwise stated. Glasgow's Modified Eagle Medium (GMEM, Sigma-Aldrich) was supplemented with 10% fetal bovine serum; 0.25% sodium bicarbonate; 0.1% non-essential amino acids; 2 mM L-glutamine; 1 mM sodium pyruvate; 0.1 mM β-mercaptoethanol; 100 U mL^{-1} leukaemia inhibitory factor (LIF).

Preparation of 0.2, 0.5 and 2 μm amino functionalised polystyrene-*co*-DVB microspheres

0.5 and 2 μm polystyrene microspheres were prepared by dispersion polymerisation as we have previously reported.[21] Briefly, AIBN (0.01 equiv.) was dissolved with VBAH (0.01 equiv.) in styrene (1 equiv.) with DVB (0.01 equiv.) and added to nitrogen degassed ethanol (or 93 : 7 ethanol–water to prepare 0.5 μm beads) with polyvinylpyrrolidone (M_w 40 000, 0.003 equiv.). The resulting solution was stirred (350 rpm) at 25 °C for 2 hours before the reaction mixture was heated to 70 °C and stirred for 18 h. The resulting microspheres were isolated by centrifugation (8500 rpm, 5–10 min) and washed sequentially with methanol and water. Microspheres were stored in sterile water at 4 °C.

0.2 μm polystyrene microspheres were prepared by emulsifier-free emulsion polymerisation as we have previously reported.[21] In brief, styrene (1 equiv.), DVB (0.02 equiv.), VBAH (0.01 equiv.) and magnesium sulfate (0.002 equiv.) were stirred in deoxygenated water for 30 min at 25 °C before heating to 80 °C and stirring at this temperature for 20 min. 2,2′-Azobis(2-amidinopropane) dihydrochloride (V-50, 0.003 equiv.) was added in a minimum volume of water and the emulsification was stirred at 80 °C for 2 h. Microspheres were subsequently isolated, washed and stored as described above.

Fluorophore labelling of amino functionalised polystyrene-*co*-DVB microspheres

0.2, 0.5 and 2 μm amino microspheres (30 mg) were washed in dimethylformamide (DMF, 3 × 1 mL) and isolated by centrifugation (13 000 rpm, 1–10 min dependent on the microsphere diameter). Fmoc-aminohexanoic acid (10 equiv.) was dissolved in DMF with 1-hydroxybenzotriazole hydrate (10 equiv.) and diisopropylcarbodiimide (10 equiv.) and stirred for 10 min at 25 °C before addition to the microspheres. The resulting suspension was mixed for 18 h at 25 °C and microspheres were then washed with DMF, methanol, water and then DMF. Fmoc deprotection was achieved *via* treatment with 20% piperidine–DMF and microspheres were subsequently washed sequentially with DMF–methanol–water. Carboxyfluorescein or Cy5-COOH (10 equiv.) was dissolved in DMF with (benzotriazol-1-yloxy)tripyrrolidinophosphonium hexafluorophosphate (PyBOP, 10 equiv.) and diisopropylethylamine (DIPEA, 10 equiv.), mixed for 1 min and then added to aminohexanoic microspheres suspended in DMF. The resulting suspension was mixed for 18 h at 25 °C and microspheres were then washed with DMF, methanol and water and finally stored in water at 4 °C.

Cell cultures

HeLa and K562 cells were cultured in RPMI; L929, HEK293T and B16F10 were cultured in DMEM; and E14Tg2A cells were cultured in GMEM on gelatine-coated flasks. Cells were grown to 70–80% confluency in a T75 flask at 37 °C/5% CO_2 prior to detachment, where appropriate, *via* trypsination. Cell pellets were collected by centrifugation (1100 rpm, 4 min) and re-suspended in the appropriate volume of culture medium before seeding onto polystyrene well plates (coated with gelatine for stem cell cultures).

Uptake of fluorophore labelled microspheres

Cells were cultured as described above in 24 well plates at a density of 3 × 10^4 cells per well. 24 h after seeding, labelled microspheres were added (86 μg mL^{-1}) and analysis was made as appropriate after 6, 12 and 24 h by flow cytometry in 0.2% trypan blue–Hank's balanced saline solution (HBSS) after cells were washed, trypsinised and centrifuged (1100 rpm, 4 min). Fluorescein fluorescence was excited using a 488 nm laser and emission collected using a 530/30 band pass filter.

Uptake under inhibition conditions

Cells were cultured as described above. Cells were pre-treated prior to the addition of microspheres with sodium azide (20 mM), mβ-CD (10 mM) with lovastatin (1 μg mL^{-1}), cytochalasin D (10 μM), DMA (10 μM), filipin III (5 μg mL^{-1}), genistein (200 μM), chlorpromazine (10 μg mL^{-1}), potassium depletion (140 mM NaCl, 20 mM Hepes, 1 mM $CaCl_2$, 1 mM $MgCl_2$, 1 mg mL^{-1} D-glucose, pH 7.4) or nocodazole (10 μg mL^{-1}) in serum-free culture media for 1 h. Microspheres were then added and incubated with cells for 3 h. Cells were washed, trypsinised and collected by centrifugation before re-suspension in 0.2% trypan blue solution for flow cytometric analysis.

Cell viability studies (MTT assay)

Cells were cultured in a 96 well plate and microspheres were added (86 μg mL^{-1} and 172 μg mL^{-1}) as described above. After 24 or 48 h the old media was removed and was replaced with phenol red-free culture media (100 μL) containing 3-(4,5-dimethylthiazol-2-yl)-2,5-diphenyltetrazolium bromide (MTT, 0.5 mg mL^{-1}). After 5 h, MTT solubilising solution (10% Triton X-100, 0.1 mol L^{-1} HCl in anhydrous isopropanol, 100 μL per well) was added to dissolve the formazan crystals and the well plate was shaken overnight at 25 °C. Absorbance was measured at 570 nm and compared to that of untreated control cells.

Microscopy of cellular uptake

Cells were cultured and fluorescein-microspheres were added as described above. Cells were washed with PBS and the nuclei stained with Hoechst 33 342 (1 μg mL^{-1}) for 10 min. Cells were then fixed with 3% *p*-formaldehyde (20 min), washed (PBS) and the actin filaments stained with AlexaFluor 568-phalloidin

(1 unit per mL) for 15 min. Cells were washed with PBS prior to microscopy in 2% fetal bovine serum–PBS or 0.2% trypan blue–HBSS.

Real-time confocal microscopy

Cells were cultured on poly-lysine coated 24 mm glass coverslips and stained with FM4-64 as according to the manufacturer's instructions (Invitrogen). Fluorescein labelled 0.5 μm microspheres were added and incubated with cells for 10 min prior to mounting the glass coverslip on a deltavision RT microscope in an incubation chamber at 37 °C/5% CO_2 (exciting microspheres using a 490/20 nm excitation filter and collecting emission using a 528/38 nm band-pass filter and exciting FM4-64 using a 555/28 nm excitation filter and collecting emission using a 617/73 nm band-pass filter). Optical slices were repeatedly scanned over 30 min.

Microscopy of lysosomes

Cells were cultured and Cy5-microspheres were added as described above. LysoTracker Red DND-99 was used according to the manufacturer's instructions (Invitrogen). Microscopic evaluation was made on a Zeiss inverted confocal DM IRE2 microscope.

RNA isolation

Cells were cultured to a density of 2×10^5 cells per well in a 6 well plate. After 24 h, unlabelled amino-microspheres were added at a concentration of 86 μg mL^{-1} and incubated with cells for 48 h. Total RNA was isolated from both HEK293T and L929 cells grown with 0.5 and 2 μm microspheres and from untreated control cells. RNA extraction was performed using an RNeasy Mini Kit according to the manufacturer's protocol (QIAGEN, UK). The integrity and concentration of the total RNA were determined using an RNA 6000 Nano Assay Kit and a Bioanalyzer 2100 according to the manufacturer's protocols (Agilent, UK).

cRNA labelling

cRNA synthesis and labelling (fluorophores Cy3 and Cy5 both from PerkinElmer/NEN Life Sciences, UK) were performed using a Low RNA Input Linear Amplification Kit according to the manufacturer's protocol (Agilent, UK). cRNA was assessed using a NanoDrop® ND-3300 fluorospectrometer (Agilent, UK).

Hybridisation and scanning

Array hybridisation was performed using both 4 × 44K Whole Human Genome microarray (design 014850, Agilent) and 4 × 44K Whole Mouse Genome (design 014868, Agilent). Array hybridisation was achieved using a Gene Expression Hybridisation Kit from (Agilent, UK). The hybridised array was washed following the post-hybridisation washing step according to the manufacturer's Gene Expression Wash Buffer Kit protocol (Agilent, UK). The dried slides were scanned on an Agilent DNA microarray scanner (G2565AA, Agilent).

Data analysis

Datasets, pre-processed by Agilent's Feature Extraction 9.1, were analysed by Genespring GX 10. Datasets were filtered by flags given by the FE software (present, marginal and absent), only samples detected as present were used for the statistical analysis.

Two different data analyses were performed. Firstly, for each cell line, the data were grouped in two datasets, one for each size (0.5 μm and 2 μm) and independently analysed against the control (untreated cells). A second analysis was performed by grouping the two datasets together to analyse the more general interaction between microspheres and cells, irrespective of microsphere size, against the control (untreated cells). T-Test statistical analyses were carried out (T-test against zero) and p-values were computed asymptotically, where p-values < 0.01 were considered significant, meaning a probability of real changes in expression of 99.9%.

Quantitative real-time PCR analysis

Quantitative real-time PCR was used to validate the effect of the cell–polymer interactions on the gene expression profile. Total RNA was isolated from both HEK293T and L929 cells grown in the presence of 0.5 μm and 2 μm microspheres and untreated control cells. RNA extraction was performed using a RNeasy Mini Kit according to the manufacturer's protocol (QIAGEN, UK). The integrity and concentration of total RNA were determined using a RNA 6000 Nano Assay Kit and a Bioanalyzer 2100 (Agilent, UK). RNA (500 ng) was used for cDNA synthesis with Superscript III (Invitrogen), according to manufacturer's instructions. Real-time RT-PCR was performed using a LightCycler 480 (Roche) and a LightCycler 480 SYBR Green 1 Master (Roche). Primers were designed with the Roche ProbeFinder online and purchased from MWG-Operon. The following cycling conditions were used: denaturation: 95 °C 5 min, amplification: 95 °C 5 s, 58 °C 10 s, 72 °C 20 s (45 cycles), acquisition: 81 °C 1 s, melting curve: 95 °C 1 s, 65 °C 10 s, 95 °C—ramp 5 °C s^{-1} continuous, cool: −40 °C 10 s. Standard curves were generated from cDNA dilutions. Data were normalised relative to human β-actin.[45] PCR primers and annealing temperature (T_a) are listed in ESI† Table SVII.

Conclusions

In conclusion, microspheres of varying diameter have been analysed for uptake in a range of cell lines with a focus on their uptake in mouse melanoma cells. Uptake was not prevented following inhibition of either ATP hydrolysis or cholesterol synthesis or scavenging, nor slowed down by inhibitors of clathrin or caveolae mediated endocytosis or non-specific uptake *via* membrane ruffling. Although uptake by endocytosis is not limited to the mechanisms analysed here, microspheres appear not to be co-localised with acidic compartments and an endosome could not be observed by real-time confocal microscopy. This suggests that microspheres likely enter cells *via* a passive, but rapid mechanism. Furthermore, gene expression profiling of human and murine cells incubated with 2 μm and 0.5 μm microspheres revealed no significant changes in gene

expression. A handful of genes showed minimal changes and none of them was associated with a cell death or toxicity pathway, supporting the notion that the microspheres' presence within the cell is remarkably well tolerated and does not result in toxicity at the genetic level.

Acknowledgements

The authors would like to thank the BBSRC and the EPSRC for funding. R.S.M. would like to thank the Royal Society for a Dorothy Hodgkin Fellowship. The authors are grateful to Maria Lopalco for the Cy5 dye.

References

1 G. J. Nabel, E. G. Nabel, Z.-Y. Yang, B. A. Fox, G. E. Plautz, X. Gao, L. Huang, S. Shu, D. Gordon and A. E. Chang, *Proc. Natl. Acad. Sci. U. S. A.*, 1993, **90**, 11307–11311.
2 J. J. Díaz-Mochón, L. Bialy, J. Watson, R. Sánchez-Martín and M. Bradley, *Chem. Commun.*, 2005, 3316–3318.
3 Z. Liu, M. Winters, M. Holodniy and H. Dai, *Angew. Chem., Int. Ed.*, 2007, **46**, 2023–2027.
4 M. J. Parnham and H. Wetzig, *Chem. Phys. Lipids*, 1993, **64**, 263–274.
5 J. M. Wörle-Knirsch, K. Pulskamp and H. F. Krug, *Nano Lett.*, 2006, **6**, 1261–1268.
6 E. Boschetti and A. Schwarz, in *Medical and Biotechnology Applications: MML Series*, ed. R. Arshady, John Wiley & Sons, New York, 2nd edn, 1999, pp. 171–189.
7 A. Bernheim and M. A. Miglierina, *Biol. Cell*, 1986, **58**, 179–182.
8 S. Slomkowski, T. Basinska and B. Miksa, *Polym. Adv. Technol.*, 2002, **13**, 905–918.
9 W. Zauner, N. A. Farrow and A. M. R. Haines, *J. Controlled Release*, 2001, **71**, 39–51.
10 J. Rejman, V. Oberle, I. S. Zuhorn and D. Hoesktra, *Biochem. J.*, 2004, **377**, 159–170.
11 S. K. Banerji and M. A. Hayes, *Langmuir*, 2007, **23**, 3305–3313.
12 D. Pantarotto, J. Briand, M. Prato and A. Bianco, *Chem. Commun.*, 2004, 16–17.
13 P. Cherukuri, S. M. Bachilo, S. H. Litovsky and R. B. Weisman, *J. Am. Chem. Soc.*, 2004, **126**, 15638–15639.
14 S. Akhtar and K. J. Lewis, *Int. J. Pharm.*, 1997, **151**, 57–67.
15 R. M. Sánchez-Martín, M. Cuttle, S. Mittoo and M. Bradley, *Angew. Chem., Int. Ed.*, 2006, **45**, 5472–5474.
16 M. Bradley, L. Alexander, K. Duncan, M. Chennaoui, A. C. Jones and R. M. Sánchez-Martín, *Bioorg. Med. Chem. Lett.*, 2008, **18**, 313–317.
17 L. M. Alexander, R. M. Sánchez-Martín and M. Bradley, *Bioconjugate Chem.*, 2009, **20**, 422–426.
18 R. M. Sánchez-Martín, L. Alexander, M. Muzerelle, J. M. Cardenas-Maestre, A. Tsakiridis, J. M. Brickman and M. Bradley, *ChemBioChem*, 2009, **10**, 1453–1456.
19 J. Ziauddin and D. M. Sabatini, *Nature*, 2001, **411**, 107–109.
20 S. Pernagallo, J. J. Díaz-Mochón and M. Bradley, *Lab Chip*, 2009, **9**, 397–403.
21 R. M. Sánchez-Martín, M. Muzerelle, N. Chitkul, S. E. How, S. Mittoo and M. Bradley, *ChemBioChem*, 2005, **6**, 1341–1345.
22 S. L. Schmid and L. L. Carter, *J. Cell Biol.*, 1990, **111**, 2307–2318.
23 K. Sandvig and S. Olsnes, *J. Biol. Chem.*, 1982, **257**, 7504–7513.
24 V. L. Mosiman, B. K. Patterson, L. Canterero and C. L. Goolsby, *Cytometry, Part B*, 1997, **30**, 151–156.
25 I. S. Zuhorn, R. Kalicharan and D. Hoekstra, *J. Biol. Chem.*, 2002, **277**, 18021–18028.
26 E. P. Kilsdonk, P. G. Yancey, G. W. Stoudt, F. W. Bangerter, W. J. Johnson, M. C. Phillips and G. H. Rothblat, *J. Biol. Chem.*, 1995, **270**, 17250–17256.
27 P. A. Orlandi and P. H. Fishman, *J. Cell Biol.*, 1998, **141**, 905–915.
28 L. Pelkmans, D. Püntener and A. Helenius, *Science*, 2002, **296**, 535–539.
29 V. Puri, R. Watanabe, R. Deep-Singh, M. Dominguez, J. C. Brown, C. L. Wheatley, D. L. Marks and R. E. Pagano, *J. Cell Biol.*, 2001, **154**, 535–548.
30 J.-S. Shin and S. N. Abraham, *Microbes Infect.*, 2001, **3**, 755–761.
31 L.-H. Wang, K. G. Rothberg and R. G. W. Anderson, *J. Cell Biol.*, 1993, **123**, 1107–1117.
32 F. M. Brodsky, C. Y. Chen, C. Knuehl, M. C. Towler and D. E. Wakeham, *Annu. Rev. Cell Dev. Biol.*, 2001, **17**, 517–568.
33 E. M. Van Dam and W. Stoorvogel, *Mol. Biol. Cell*, 2002, **13**, 169–182.
34 S. Grimmer, B. Van Deurs and K. Sandvig, *J. Cell Sci.*, 2002, **115**, 2953–2962.
35 J. W. Murray and A. W. Wolkoff, *Adv. Drug Delivery Rev.*, 2003, **55**, 1385–1403.
36 S. C. Silverstein, R. M. Steinman and Z. A. Cohn, *Annu. Rev. Biochem.*, 1977, **46**, 669–722.
37 J. M. Hall, C. C. Parrish and R. J. Thompson, *Biol. Bull.*, 2002, **202**, 201–203.
38 W. J. Betz, F. Mao and C. B. Smith, *Curr. Opin. Neurobiol.*, 1996, **6**, 365–371.
39 D. R. Trollinger, W. E. Cascio and J. J. Lemasters, *Biophys. J.*, 2000, **79**, 39–50.
40 D. B. Wheeler, A. E. Carpenter and D. M. Sabatini, *Nat. Genet.*, 2005, **37**, S25–30.
41 V. Baldacchino, S. Oble, P. O. Décarie, I. Bourdeau, P. Hamet, J. Tremblay and A. Lacroix, *J. Mol. Endocrinol.*, 2005, **35**, 1–12.
42 X. Du, M. R. Rao, X. Q. Chen, W. Wu, S. Mahalingam and D. Balasundaram, *Mol. Biol. Cell*, 2006, **17**, 1–13.
43 T. Tsukihara, H. Aoyama, E. Yamashita, T. Tomizaki, H. Yamaguchi, K. Shinzawa-Itoh, R. Nakashima, R. Yaono and S. Yoshikawa, *Science*, 1996, **272**, 1136–1144.
44 B. D. Spiegelberg, J. Dela Cruz, T. H. Law and J. D. York, *J. Biol. Chem.*, 2005, **280**, 5400–5405.
45 V. S. Subramanian, Z. M. Mohammed, A. Molina, J. S. Marchant, N. D. Vaziri and H. M. Said, *J. Physiol.*, 2007, **582**, 73–85.